The Flavivirus Precursor Membrane-Envelope Protein Complex: Structure and Maturation

Long Li, *et al.*

Science **319**, 1830 (2008);
DOI: 10.1126/science.1153263

vae (table S1, ArrayExpress accession number E-MEXP-1394). This revealed a battery of differentially expressed genes associated with lipid transport, hormonal regulation, posttranslational modification, protein turnover, ribosomal biogenesis, energy transfer, and other physiometabolic processes, as well as a number of novel, possibly *Apis*-specific genes with unknown functions (table S1). One differentially expressed gene predicted to encode an ortholog of the adenosine triphosphatase (ATPase) Belphegor has been shown in *Drosophila* to be regulated by TOR, a serine/threonine kinase that is central to a signaling cascade controlling growth (*27*). TOR is believed to be at the core of an ancient gene network that senses nutrient levels, and its involvement in honeybee queen development has already been considered (*7*, *28*). We also expected that the set of genes responsive to Dnmt3 silencing might contain genes implicated in chromatin remodeling and integrity. It is known that regulation of eukaryotic gene expression requires two classes of chromatin-remodeling enzymes: those that modify histones through acetylation, phosphorylation, or methylation and those that alter chromatin structure through hydrolysis of adenosine triphosphate (ATP) (*29*). From the list shown in table S1, we identified at least two genes belonging to this category, a subunit of the INO80 nucleosome remodeling complex and an ATPase of the type involved in structural maintenance of chromosomes. The transcriptional responses to Dnmt3 silencing are in good agreement with our previous study in which we used a smaller, expressed sequence tag (EST)–based array to compare gene expression between queen and worker larvae extracted from the colony environment (*7*). Thus, both Dnmt3 silencing and feeding with royal jelly induce reprogramming of the larval transcriptome that is characterized by transcriptional shift toward higher expression of physiometabolic genes, including genes coding for metabolic enzymes and the general growth of the organism.

This study shows that in *A. mellifera* DNA methylation is a key component of an epigenetic network controlling a most important aspect of eusociality, the reproductive division of labor (*30*). Further work is required to unravel the causal relation between diet-induced methylation changes and altered gene expression, but our data hold substantial promise for functional methylome analyses in Metazoa using an easily manipulatable insect system. Where appropriate, the relevance of the honeybee findings to mammals can be evaluated to determine the level of data transferability, especially in the context of nutritional processes, longevity, and even drug treatment. Methylation data on a genomic scale combined with genomewide expressional profiling in both social and solitary insects possessing functional CpG methylation systems will be needed to dissect the intricacies of this elaborate regulatory system.

References and Notes

1. M. West-Eberhard, *Annu. Rev. Ecol. Syst.* **20**, 249 (1989).
2. M. J. West-Eberhard, *Developmental Plasticity and Evolution* (Oxford Univ. Press, New York, 2003).
3. E. O. Wilson, *Proc. Am. Philos. Soc.* **123**, 204 (1979).
4. K. Hartfelder, W. Engels, *Curr. Top. Dev. Biol.* **40**, 45 (1998).
5. J. D. Evans, D. E. Wheeler, *Proc. Natl. Acad. Sci. U.S.A.* **96**, 5575 (1999).
6. J. D. Evans, D. E. Wheeler, *Genome Biol.* **2**, 1 (2000).
7. A. R. Barchuk *et al.*, *BMC Dev. Biol.* **7**, 70 (2007).
8. E. H. Colhoun, M. V. Smith, *Nature* **188**, 854 (1960).
9. R. W. Shuel, S. E. Dixon, *Insectes Soc.* **7**, 265 (1960).
10. N. Weaver, *Ann. Entomol. Soc. Am.* **50**, 283 (1957).
11. N. Weaver, *J. Econ. Entomol.* **50**, 759 (1957).
12. R. Jaenisch, A. Bird, *Nat. Genet.* **33** (suppl.), 245 (2003).
13. G. C. Burdge, M. A. Hanson, J. L. Slater-Jefferies, K. A. Lillycrop, *Br. J. Nutr.* **97**, 1036 (2007).
14. G. Kaati, L. O. Bygren, S. Edvinsson, *Eur. J. Hum. Genet.* **10**, 682 (2002).
15. R. A. Waterland, R. L. Jirtle, *Mol. Cell. Biol.* **23**, 5293 (2003).
16. V. K. Rakyan, M. E. Blewitt, R. Druker, J. I. Preis, E. Whitelaw, *Trends Genet.* **18**, 348 (2002).
17. I. C. Weaver *et al.*, *Nat. Neurosci.* **7**, 847 (2004).
18. M. G. Goll, T. H. Bestor, *Annu. Rev. Biochem.* **74**, 481 (2005).
19. Y. Wang *et al.*, *Science* **314**, 645 (2006).
20. M. Schaefer, F. Lyko, *Bioessays* **29**, 208 (2007).
21. Materials and methods are available on *Science* Online.
22. J. Maleszka, S. Forêt, R. Saint, R. Maleszka, *Dev. Genes Evol.* **217**, 189 (2007).
23. FlyAtlas, http://flyatlas.org/atlas.cgi?name=FBgn0033206.
24. GEO (Gene Expression Omnibus), www.ncbi.nlm.nih.gov/sites/entrez?db=geo&cmd=search&term=FBgn0033206
25. J. A. Nelson, *The Embryology of the Honeybee* (Princeton Univ. Press, Princeton, NJ, 1915).
26. G. M. Ulrich, H. Rembold, *Cell Tissue Res.* **230**, 49 (1983).
27. D. A. Guertin, K. V. Guntur, G. W. Bell, C. C. Thoreen, D. M. Sabatini, *Curr. Biol.* **16**, 958 (2006).
28. A. Patel *et al.*, *PLoS ONE* **2**, e509 (2007).
29. C. J. Fry, C. L. Peterson, *Science* **295**, 1847 (2002).
30. M. D. Drapeau, S. Albert, R. Kucharski, C. Prusko, R. Maleszka, *Genome Res.* **16**, 1385 (2006).
31. J. Maindonald, J. Braun, *Data Analysis and Graphics Using R* (Cambridge Univ. Press, Cambridge, 2007).

32. We thank G. Miklos for stimulating discussion and comments on the manuscript and P. Helliwell for beekeeping and excellent technical assistance. This work was supported by the Australian Research Council Discovery grant DP0770821 awarded to R.M. GenBank accession no. for *dynactin p62* is XP_001121083.

Supporting Online Material

www.sciencemag.org/cgi/content/full/1153069/DC1
Materials and Methods
Figs. S1 to S4
Tables S1 and S2
References

16 November 2007; accepted 27 February 2008
Published online 13 March 2008;
10.1126/science.1153069
Include this information when citing this paper.

The Flavivirus Precursor Membrane-Envelope Protein Complex: Structure and Maturation

Long Li, Shee-Mei Lok, I-Mei Yu, Ying Zhang, Richard J. Kuhn, Jue Chen, Michael G. Rossmann*

Many viruses go through a maturation step in the final stages of assembly before being transmitted to another host. The maturation process of flaviviruses is directed by the proteolytic cleavage of the precursor membrane protein (prM), turning inert virus into infectious particles. We have determined the 2.2 angstrom resolution crystal structure of a recombinant protein in which the dengue virus prM is linked to the envelope glycoprotein E. The structure represents the prM-E heterodimer and fits well into the cryo–electron microscopy density of immature virus at neutral pH. The pr peptide β-barrel structure covers the fusion loop in E, preventing fusion with host cell membranes. The structure provides a basis for identifying the stages of its pH-directed conformational metamorphosis during maturation, ending with release of pr when budding from the host.

Many viruses, including flaviviruses (*1*), undergo a maturation step immediately before their release from the host; the evident purpose of this step is to maintain stability for the hazardous transfer to a new host while preparing virions for rapid fusion with, and entry into, a cell. Flaviviruses within the *Flaviviridae* family are major human pathogens that include dengue virus, West Nile virus, yellow fever virus, and Japanese encephalitis virus. They have a positive-sense, 11-kb RNA genome that is packaged together with multiple copies of the capsid protein within a lipid envelope (*2*). The genome is translated as a polyprotein that has the capsid protein, the precursor membrane glycoprotein (prM), and the envelope glycoprotein (E) in its N-terminal region (Fig. 1A). The polyprotein is cleaved into component proteins by viral and cellular proteases (*2*). Partially assembled flavivirus nucleocapsids bud from the endoplasmic reticulum, thereby becoming enveloped with a lipid membrane that carries with it the E and prM glycoproteins (*2*). These immature particles are transported through the cellular secretory pathway, where the cellular furin protease cleaves prM, eventually resulting in the release of the pr peptide and formation of mature virions (*3*, *4*).

The dengue virus prM glycoprotein consists of 166 amino acids. Cleavage by furin releases

Department of Biological Sciences, Purdue University, West Lafayette, IN 47907, USA.

*To whom correspondence should be addressed. E-mail: mr@purdue.edu

the N-terminal 91 "pr" residues during maturation, leaving only the ectodomain (residues 92 to 130) and C-terminal transmembrane region (residues 131 to 166) of "M" in the virion. The pr peptide protects immature virions against premature fusion with the host membrane (*5*, *6*). The dengue virus E glycoprotein participates in the fusion of the virion with the endosomal membrane at low pH. It consists of an ectodomain (soluble E protein, sE), a stem region, and a transmembrane domain. The x-ray crystallographic structure of sE has been determined for a number of flaviviruses (*7*–*12*), all of which have three domains (DI, DII, and DIII) that consist mainly of β sheets with the fusion loop at the distal end of DII. The E protein is able to switch among different oligomeric states: as a trimer of prM-E heterodimers in immature particles, as a dimer in mature virus, and as a trimer when fusing with a host cell (*8*, *10*).

The cryo–electron microscopy (cryoEM) structures of immature flaviviruses have been determined at neutral pH (*6*, *13*). The "spiky" icosahedral immature virions have a diameter of about 600 Å and contain 60 trimeric prM-E spikes. In contrast, the final "smooth"-surfaced icosahedral mature particles have a diameter of about 500 Å and contain 90 E dimers arranged in a herringbone pattern and 180 copies of the M protein (*14*, *15*). The transformation from immature to mature particles requires some large rearrangement of the E and M proteins (Fig. 2) (*12*, *13*).

A recombinant fusion protein of prM and E from dengue virus 2 was constructed in which the transmembrane region of prM was replaced with an 8–amino acid linker (Fig. 1B) (*16*). The furin cleavage site of prM was mutated to prevent cleavage of the recombinant protein by intracellular proteases. The crystal structure of the recombinant protein was determined at pH 5.5 to 2.20 Å resolution, and also at pH 7.0 to 2.60 Å resolution (table S1). There were no significant structural differences between the two determinations, which had a root mean square difference of 1.0 Å between all pairs of equivalent atoms. Because of the slightly higher resolution of the low-pH structure, it was chosen for all subsequent calculations and discussions. The polypeptide chain of much of the prM protein (residues 1 to 81, corresponding to most of the pr peptide) and most of the sE protein could be traced in the electron density of the prM-E crystal structure. The pr peptide was positioned over the fusion loop at the distal end of DII (Fig. 3A), as anticipated given that it functions to prevent membrane fusion (*5*).

The pr peptide consists of seven β strands that are mostly antiparallel (Fig. 3). Three disulfide bonds (C34-C68, C45-C80, and C53-C66) stabilize the pr peptide structure, and the electron density map shows that Asn^{69} is glycosylated. A DALI search (*17*) did not find any structures with significant similarity to that of the pr peptide. The structure of the E protein in

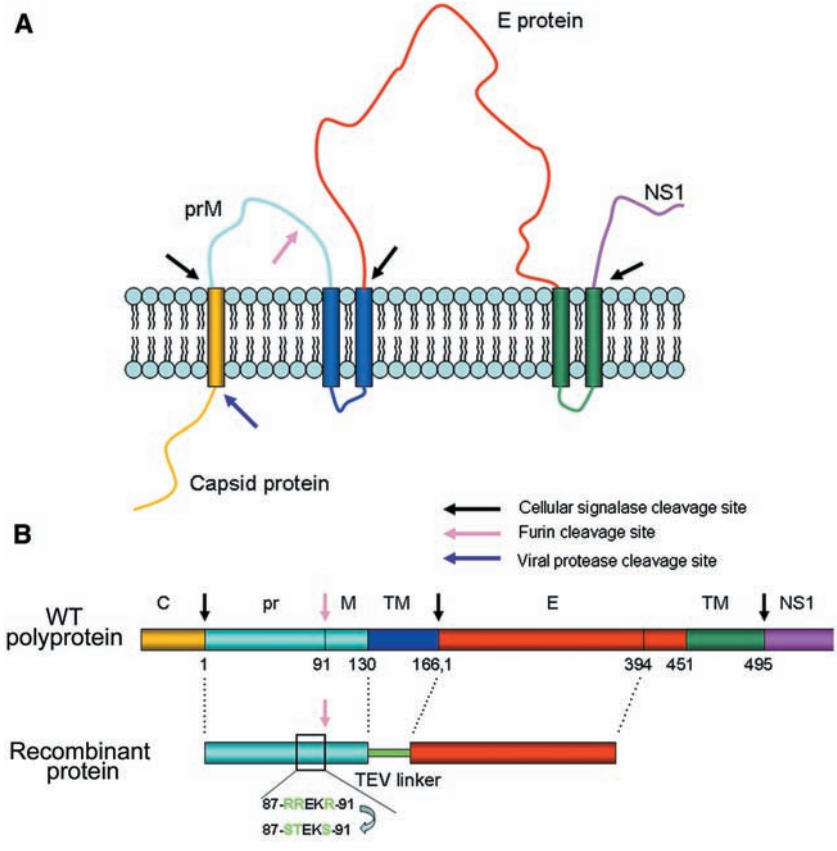

Fig. 1. The dengue virus polyprotein and the recombinant protein containing the prM and E proteins. (**A**) Threading of the dengue virus polyprotein N-terminal region through the endoplasmic reticulum membrane, showing the positions of the capsid, prM, and E structural proteins. Different-colored arrows indicate various protease cleavage sites. (**B**) The order of viral proteins in the wild-type polyprotein and in the recombinant protein construct. The proteins are identified by the same colors as in (A). The mutations to inhibit furin cleavage in the recombinant protein are shown below (*21*). The linker between the prM and E proteins is labeled TEV.

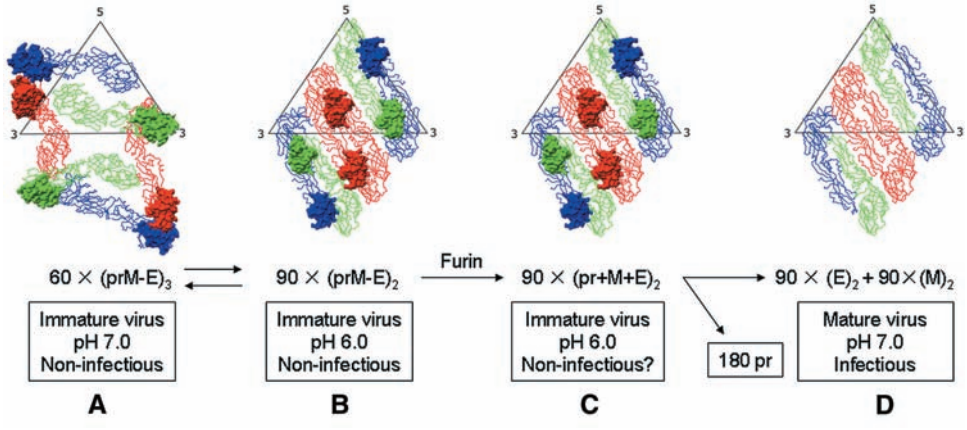

Fig. 2. Rearrangement of the prM and E proteins during virus maturation. (**A** to **D**) Sequence of events as referenced in the text. The E proteins are shown as a Cα backbone; space-filling atoms show the pr peptide surfaces. The three independent heterodimers per icosahedral asymmetric unit are colored red, green, and blue. Although the diagram assumes knowledge of the relationship among the positions of specific heterodimers in the immature and mature viruses (red goes to red, green to green, and blue to blue), this is not known.

the prM-E heterodimer is similar to the crystal structure of the E protein in the dimeric, prefusion form (*12*). The hinge angle between DI and DII is only 5° different from the structure of E in immature virus (*12*), as compared to 23° with the mature virus, which suggests that the oligomeric state of the E protein determines the hinge angle. This similarity supports the biological relevance of the recombinant fusion protein structure. The contact area between pr and E is 865 Å^2, representing 16% of the surface area of pr and 4% of E. There are three prominent complementary electrostatic patches (Fig. 3C) involving (Arg^6), (Glu^{46}, Asp^{47}), and (Asp^{63}, Asp^{65}) on pr, and involving (Glu^{84}), (Lys^{64}), and (His^{244}, Lys^{247}) on E (table S2), respectively. Of these, the pr residues Asp^{63} and Asp^{65} and the E residue His^{244} are strictly conserved among all known flavivirus sequences.

A pseudo-atomic structure of the immature dengue virus at neutral pH (fig. S1A) was generated by fitting the prM-E crystal structure into the 12.5 Å resolution cryoEM density map (*12*). The structure of the pr peptide fits the density well, including the prominent carbohydrate moieties at residue Asn^{69} (fig. S1B and table S3). The surface area buried between pairs of heterodimers is 1052 Å^2, 1445 Å^2, and 0 Å^2 in the "blue-red," "red-green," and "green-blue" interfaces, respectively, showing nonequivalent contacts between each of the three pairs of heterodimers (Fig. 4 and fig. S1). The hydrophobic fusion loop in each of the three E proteins within one spike is covered and surrounded by loops of the pr peptides and the carbohydrate moieties associated with Asn^{69} in pr, thus making the surface of the immature particle more hydrophilic (Fig. 4B) and protecting the E protein from premature fusion.

The cryoEM density representing the surface spikes was set to zero at all points within 3.0 Å of every atom in the fitted x-ray structure. There then remained traces of density that ran along the edge of each E molecule toward the lipid membrane (fig. S1C and fig. S2, A to C). These density traces were positioned similarly on each E molecule, in agreement with density in the crystal structure that had been presumed to be the N-terminal region of the M protein (fig. S2D) (*16*). The trace of the M protein suggested that the pr polypeptide chain is extended linearly along the surface of the E protein, mostly on the inside of the spike (fig. S1C). The position of the furin cleavage site could be reasonably well inferred by building an extended polypeptide chain into the density traces representing the junction of the pr peptide with the M protein (Fig. 4C and movie S1). Docking of the known structure of furin (*18*) onto the cleavage site showed that furin would be sterically hindered from binding to any of the three prM-E heterodimers within a spike, thereby demonstrating why furin is unable to

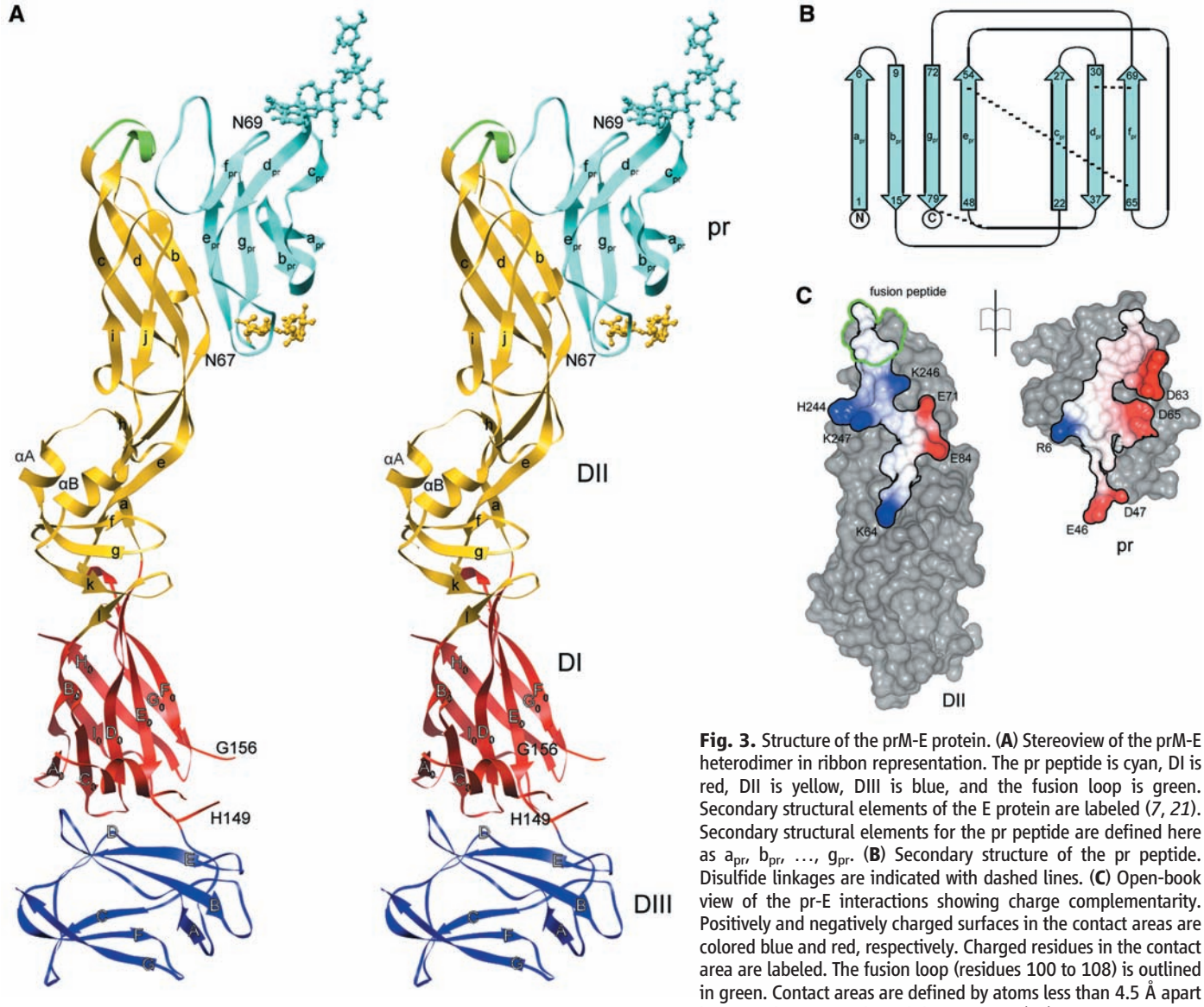

Fig. 3. Structure of the prM-E protein. (**A**) Stereoview of the prM-E heterodimer in ribbon representation. The pr peptide is cyan, DI is red, DII is yellow, DIII is blue, and the fusion loop is green. Secondary structural elements of the E protein are labeled (*7*, *21*). Secondary structural elements for the pr peptide are defined here as a_{pr}, b_{pr}, …, g_{pr}. (**B**) Secondary structure of the pr peptide. Disulfide linkages are indicated with dashed lines. (**C**) Open-book view of the pr-E interactions showing charge complementarity. Positively and negatively charged surfaces in the contact areas are colored blue and red, respectively. Charged residues in the contact area are labeled. The fusion loop (residues 100 to 108) is outlined in green. Contact areas are defined by atoms less than 4.5 Å apart between the pr peptide and the E protein (*21*).

cleave the pr polypeptide in the immature virus at neutral pH (*4*).

The accompanying paper (*4*) shows that low-pH immature virus particles (Fig. 2B) have a structure in which the arrangement of the E proteins is essentially the same as that of the mature virus (Fig. 2D). However, the interface between the DII domains in the E dimer is in part the same surface where the extended polypeptide of the M protein binds in the neutral-pH immature virus (fig. S3A). Thus, if the M protein were in the conformation as found in the immature virus at neutral pH, it would sterically block the formation of the E dimer. Hence, the conformation of M must be different in the low-pH immature virus, consistent with its apparent flexibility in the crystal structure of the heterodimer and also consistent with the changed position of the M protein's transmembrane helices during maturation (fig. S3) (*15*). Indeed, the low-pH conformation, unlike the neutral-pH conformation of the M protein, has been found to be accessible to furin cleavage (*4*).

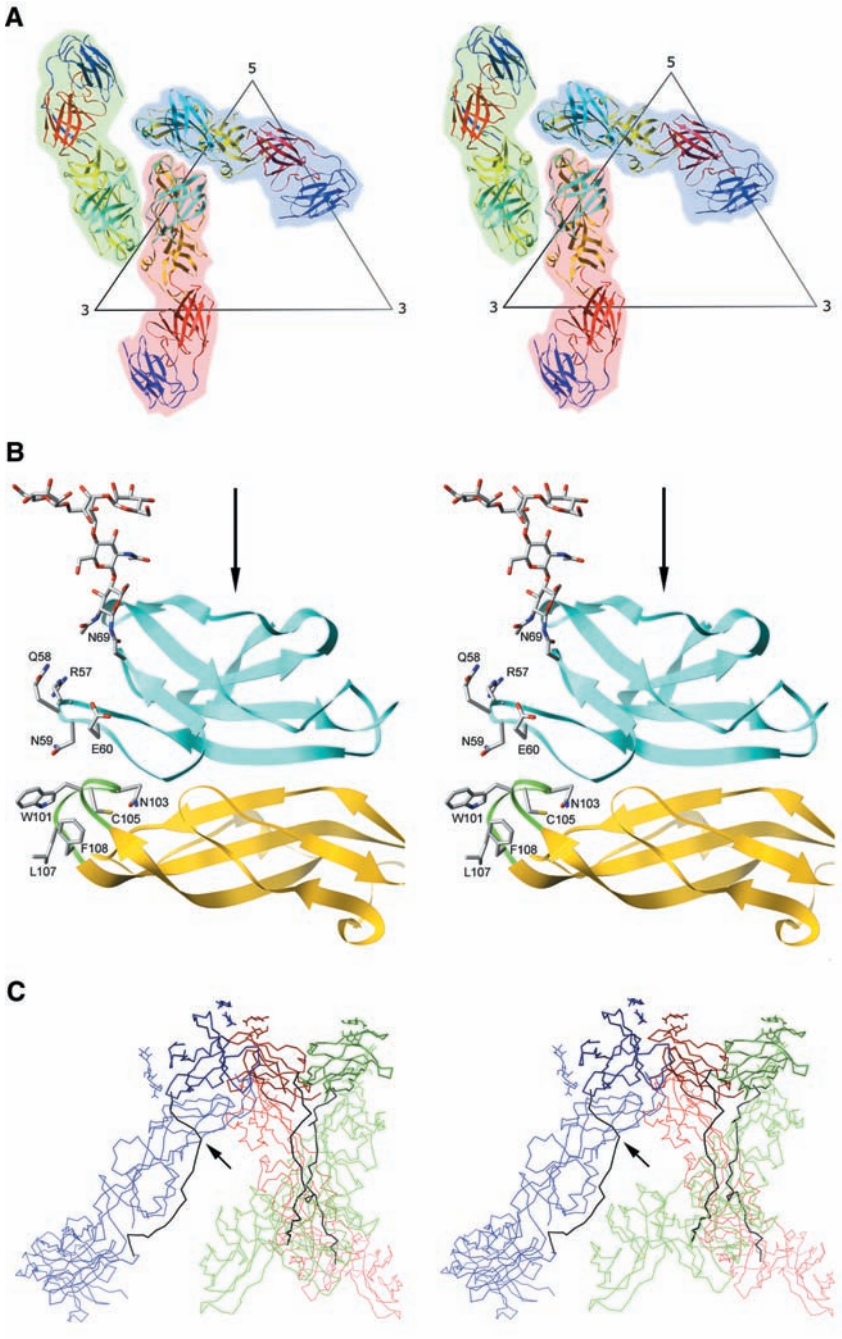

Fig. 4. Pseudo-atomic structure of the neutral-pH immature dengue virus. (**A**) Stereoview of one spike of the immature virus as seen from outside the virus, colored as in Fig. 3A. The background to each heterodimer is colored red, green, or blue in accordance with the color code used in Fig. 2 and table S3. (**B**) Stereoview showing the fusion loop of the E molecule and the protecting pr loops and glycans (*21*). The arrow indicates the direction of viewing from outside the virus. (**C**) Stereoview of the fitted pr-E Cα backbones with the Cα trace of the extended M polypeptide (black) running along the edge of each E protein. The Cα backbones of the pr peptides are in bold. The approximate site of furin cleavage is marked with a black arrow in the blue molecule.

The large conformational change that occurs when the immature virus changes from the neutral-pH to the low-pH form was found to be reversible for dengue virus (Fig. 2, A and B), as long as prM was still intact (*4*). However, once prM had been cleaved (Fig. 2C), there was no further conformational change when the pH was returned to neutral (Fig. 2, C and D); instead, the cleaved pr peptide was released (*4*). Apparently the extended polypeptide of the M protein, along the side of the E protein (Fig. 4C and fig. S2), is essential for maintaining the reversibility of the conformational change (Fig. 2, A and B). An analogy might be the effect of a drawstring that opens and closes a curtain. Once the string (i.e., the M protein) is cut (i.e., furin cleavage), there can be no further movement. Mutating a conserved histidine residue to alanine in the M protein (His^{99} → Ala) in Japanese encephalitis virus inhibits the formation of prM-E heterodimers (*19*). The corresponding residue, His^{98} in dengue virus, is located approximately in the center of the extended M protein, opposite the hydrophobic surfaces of helices αA and αB in the E protein. Thus, a change of pH might alter the interactions between M and E, leading to the transition between the "spiky" and "smooth" virus conformations.

On one hand, pr remains bound to E when the immature low-pH virus is returned to neutral pH, thus protecting the immature virus against fusion. On the other hand, after cleavage of M, pr is released from E to activate the virus when returning the pH to neutral. The average area of contact between a pr peptide and an E protein in a spike of the immature virus at neutral pH is slightly larger than the area of contact in the immature virus at low pH (table S4). Thus, not only is each pr peptide tethered covalently to the M protein, but also the pr peptide probably has a slightly greater affinity for the trimeric E protein spike of immature virus at neutral pH relative to the dimeric smooth surface of mature virus. In contrast, His^{244} of the E protein is highly conserved and is situated in the prM-E interface opposite the completely conserved Asp^{63} of the pr peptide (Fig. 3C), causing the affinity of the pr peptide for the E protein to decrease when the pH is raised to neutral. This would allow the pr peptide to be released at neutral pH from the dimeric E structure, but only when the pr peptide has been cleaved. As evolution is highly conservative of structure (*20*), the maturation process described here for dengue virus is likely to have structural homologies in other enveloped viruses.

References and Notes

1. S. Mukhopadhyay, R. J. Kuhn, M. G. Rossmann, *Nat. Rev. Microbiol.* **3**, 13 (2005).
2. B. D. Lindenbach, C. M. Rice, in *Fields Virology*, D. M. Knipe, P. M. Howley, Eds. (Lippincott Williams & Wilkins, Philadelphia, 2001), pp. 991–1041.
3. K. Stadler, S. L. Allison, J. Schalich, F. X. Heinz, *J. Virol.* **71**, 8475 (1997).
4. I.-M. Yu *et al.*, *Science* **319**, 1834 (2008).
5. F. Guirakhoo, R. A. Bolin, J. T. Roehrig, *Virology* **191**, 921 (1992).
6. Y. Zhang *et al.*, *EMBO J.* **22**, 2604 (2003).
7. F. A. Rey, F. X. Heinz, C. Mandl, C. Kunz, S. C. Harrison, *Nature* **375**, 291 (1995).
8. S. Bressanelli *et al.*, *EMBO J.* **23**, 728 (2004).
9. Y. Modis, S. Ogata, D. Clements, S. C. Harrison, *Proc. Natl. Acad. Sci. U.S.A.* **100**, 6986 (2003).
10. Y. Modis, S. Ogata, D. Clements, S. C. Harrison, *Nature* **427**, 313 (2004).
11. R. Kanai *et al.*, *J. Virol.* **80**, 11000 (2006).
12. Y. Zhang *et al.*, *Structure* **12**, 1607 (2004).
13. Y. Zhang, B. Kaufmann, P. R. Chipman, R. J. Kuhn, M. G. Rossmann, *J. Virol.* **81**, 6141 (2007).
14. R. J. Kuhn *et al.*, *Cell* **108**, 717 (2002).
15. W. Zhang *et al.*, *Nat. Struct. Biol.* **10**, 907 (2003).
16. See supporting material on *Science* Online.
17. L. Holm, C. Sander, *Science* **273**, 595 (1996).
18. S. Henrich *et al.*, *Nat. Struct. Biol.* **10**, 520 (2003).
19. Y.-J. Lin, S.-C. Wu, *J. Virol.* **79**, 8535 (2005).
20. M. G. Rossmann, D. Moras, K. W. Olsen, *Nature* **250**, 194 (1974).
21. Single-letter abbreviations for amino acid residues: A, Ala; C, Cys; D, Asp; E, Glu; F, Phe; G, Gly; H, His; I, Ile; K, Lys; L, Leu; M, Met; N, Asn; P, Pro; Q, Gln; R, Arg; S, Ser; T, Thr; V, Val; W, Trp; Y, Tyr.

22. We thank Y. Xiang and W. Zhang for many helpful discussions; S. Kelly and C. Towell for help in the preparation of the manuscript; and the staff at APS GM/CA sector for their help in data collection. The facilities are supported by the U.S. Department of Energy and/or NIH. The work was supported by NIH program project grant AI055672 (R.J.K., M.G.R., J.C.) and National Institute of Allergy and Infectious Diseases Region V Great Lakes Center of Excellence for Biodefense and Emerging Infectious Diseases Research Program award 1-U54-AI-057153 (R.J.K., M.G.R.). The coordinates of the prM-E heterodimer crystal structures at pH 5.5 and 7.0 have been deposited with the Protein Data Bank (accession numbers 3C5X and 3C6E, respectively). The fit of the prM-E heterodimer into the cryoEM reconstruction of the dengue immature virus at neutral pH has been deposited with the RCSB Protein Database (accession number 3C6D).

Supporting Online Material

www.sciencemag.org/cgi/content/full/319/5871/1830/DC1
Materials and Methods
Figs. S1 to S3
Tables S1 to S4
Movie S1
References

21 November 2007; accepted 29 February 2008
10.1126/science.1153263

Structure of the Immature Dengue Virus at Low pH Primes Proteolytic Maturation

I-Mei Yu, Wei Zhang, Heather A. Holdaway, Long Li, Victor A. Kostyuchenko, Paul R. Chipman, Richard J. Kuhn, Michael G. Rossmann, Jue Chen*

Intracellular cleavage of immature flaviviruses is a critical step in assembly that generates the membrane fusion potential of the E glycoprotein. With cryo–electron microscopy we show that the immature dengue particles undergo a reversible conformational change at low pH that renders them accessible to furin cleavage. At a pH of 6.0, the E proteins are arranged in a herringbone pattern with the pr peptides docked onto the fusion loops, a configuration similar to that of the mature virion. After cleavage, the dissociation of pr is pH-dependent, suggesting that in the acidic environment of the trans-Golgi network pr is retained on the virion to prevent membrane fusion. These results suggest a mechanism by which flaviviruses are processed and stabilized in the host cell secretory pathway.

The structure of viruses is dynamic because major conformational changes are necessary for the virus to enter and disassemble in a host cell. Whereas such conformational change is triggered by receptor binding or acidification, the origin of the labile conformation is generated in the assembly pathway. For example, glycoproteins of many enveloped viruses are synthesized as inactive precursors that require proteolytic cleavage to prime their membrane fusion potential. In the case of class I fusion proteins, represented by influenza virus hemagglutinin (HA), cleavage of the HA0 precursor generates a metastable form that undergoes a low-pH-induced conformational change to facilitate membrane fusion with a host cell (*1*). In contrast, class II fusion proteins, found in flaviviruses and alphaviruses, fold cotranslationally with an auxiliary protein. Proteolytic activation involves cleavage of the auxiliary protein that is thought to free the fusion protein for subsequent conformational changes necessary for membrane fusion (*2*–*4*).

In the endoplasmic reticulum (ER) of an infected cell, newly assembled immature flaviviruses contain heterodimers of the auxiliary precursor membrane (prM) protein and the envelope (E) protein (*5*). Furin (*6*), a cellular protease primarily located in the trans-Golgi network (TGN), cleaves prM to generate mature particles where the pr peptides are released and the E proteins form homodimers (*7*, *8*). Crystal structures of the E protein at neutral pH (*7*, *9*–*12*) show that each polypeptide chain contains three domains: the structurally central domain (DI), the dimerization domain containing the fusion loop (DII), and the carboxy-terminal immunoglobulin-like domain (DIII). In the postfusion conformation observed at the endosomal pH, the E dimers rearrange into homotrimers, of which the fusion loops and the C-terminal membrane anchors are located at the same end (*13*, *14*). Thus, the membrane fusion process of flaviviruses appears to require dissociation of the E dimers and formation of the postfusion trimers.

Acidotropic reagents such as NH_4Cl that raise the pH of the TGN prevent furin cleavage, resulting in immature particles containing uncleaved prM molecules (*15*–*17*). Whereas the mature virion has a smooth surface on which 90 E dimers form a closely packed protein shell with a herringbone pattern (*8*), at neutral pH the immature particles propagated in the presence of NH_4Cl contain 60 prominent spikes, each consisting of a trimer of prM-E heterodimers (*18*, *19*). To address whether these particles are physiologically relevant, we subjected dengue virus immature particles to furin cleavage at various pH values (*20*). In agreement with previous work (*6*), prM could be cleaved only under acidic conditions (pH of 5.0 to 6.0) (Fig. 1A). Whereas uncleaved immature viruses at both pH = 8.0 and pH = 6.0 are mildly infectious, in vitro furin cleavage led to a 1000-fold increase in infectivity (Fig. 1B). Because the optimum enzymatic activity of furin was observed around neutral pH (fig. S1), the pH dependence of the cleavage likely reflects the accessibility of the cleavage sites on the viral surface, suggesting that the conformation of the immature virion at low pH is distinct from that of the neutral pH form (*18*).

Cryo–electron microscopy (cryo-EM) and image reconstruction show that immature dengue particles undergo a reversible conformational change at low pH (Fig. 1C). As previously reported (*18*, *19*), at pH = 8.0 the particles have a spiky surface with 60 icosahedrally arranged protrusions. Incubation at pH = 6.0 resulted in particles with a much smoother surface. The size of these particles was around 530 Å in diameter, which is substantially smaller than that of the neutral-pH immature form (600 Å). When back-neutralized to pH = 7.5, the smooth particles at low pH were converted to the spiky form, indicating that the pH effect is reversible. The reversibility of the conformational change was further demonstrated by in vitro furin activation experiments (fig. S2). No furin cleavage or activation was observed at pH = 7.5 for samples exposed to low pH and then back-neutralized. However, when the pH was again lowered, the particles could be activated by furin (fig. S2A). These results are consistent with the observation that the neutral-pH structures of West Nile virus

Department of Biological Sciences, 915 West State Street, Purdue University, West Lafayette, IN 47907–2054, USA.

*To whom correspondence should be addressed. E-mail: chenjue@purdue.edu